

STRUCTURE OF PYROPHYLLITE

by

J. H. RAYNER and G. BROWN

Rothamsted Experimental Station, Harpenden, Herts, England

ABSTRACT

PYROPHYLLITE gives a diffraction pattern consisting of sharp and diffuse reflections. The unit cell for all the reflections is monoclinic with $a = 5.17 \text{ \AA}$, $b = 8.92 \text{ \AA}$, $c = 18.66 \text{ \AA}$, $\beta = 99.8^\circ$. From the absences, the space group is either $C2/c$ or Cc but there are additional absences of hkl reflections with $h \neq 3n$ and l even. The additional systematic absences show that the structure is partially disordered, the disordered state being based on a small subcell defined by the sharp reflections. This subcell is monoclinic with $a' = a = 5.17 \text{ \AA}$, $b' = b/3 = 2.97 \text{ \AA}$, $c' = c/2 = 9.33 \text{ \AA}$, $\beta' = \beta = 99.8^\circ$ and belongs either to the space group Cm or $C2/m$. Co-ordinates have been found in the space group $C2/m$ by Fourier and least-squares methods, which give $R = 0.180$ for $h0l$ reflections and $R = 0.148$ for hkl reflections with $h = 0, 1, 2$. The Si—O tetrahedra are twisted 10° – 10.5° from the 'ideal' arrangement, leading to a ditrigonal array of oxygens on the surfaces of the layers. The average Si—O bond length is 1.610 \AA and the average octahedral site—O distance is 2.025 \AA . The surfaces of the layers can come together in three ways; the O—O contacts for any pair of layers are either approximately parallel to (010) with contacts 2.890 \AA and 3.028 \AA alternately or approximately parallel to planes making angles of $\pm 120^\circ$ with (010) with contacts 3.009 \AA , 3.066 \AA , 3.009 \AA , 3.343 \AA sequentially.

INTRODUCTION

STRUCTURES of layer silicate clay minerals are usually deduced from the structures of better crystallized analogous minerals. Modern methods have been used to determine the structures of vermiculite (Mathieson and Walker, 1954; Mathieson, 1958), dickite (Newnham and Brindley, 1956; Newnham, 1961), prochlorite and corundophyllite (Steinfink, 1958 a and b), amesite (Steinfink and Brunton, 1956), kaolinite (Drits and Kashaev, 1960), xanthophyllite (Takéuchi and Sadanaga, 1959), muscovite (Radoslovich, 1960), phlogopite (Steinfink, 1962), Cr-chlorite (Brown and Bailey, 1963) and ferriannite (Morimoto, Donnay, Takeda, and Donnay, 1963). Of the basic model structures for clay minerals, those of talc and pyrophyllite have not been studied since the work of Hendricks (1938, 1940).

There are two other reasons why the structure of pyrophyllite is of interest:

1. Information on the structural disorder in pyrophyllite will to some extent be applicable to the disorder which is common in clay minerals. This cannot be obtained from structure determinations of fully ordered materials.

2. Modern structure determinations have shown that the dimensional misfit between the tetrahedral and octahedral layers in dioctahedral structures is relieved mainly by the distortion of the ideal hexagonal array of surface oxygens to a ditrigonal arrangement that reduces the size of the tetrahedral layer. In the structures determined so far, features other than the misfit of the tetrahedral and octahedral units influence the structure. In micas, interlayer cations, and in minerals of the kaolinite group, hydrogen bonds between layers and across the surface of layers, affect the structure. In pyrophyllite, the tetrahedral and octahedral layers are free to come to a mutually satisfactory arrangement.

Pyrophyllite and talc both show structural disorder and give X-ray diffraction patterns consisting of sharp and diffuse reflections. This paper reports the determination of the ideally disordered structure of pyrophyllite by the analysis of the intensities of the sharp subcell reflections, using modern methods to find the atomic co-ordinates. The next step will be the choice of chemically feasible structures compatible with the ideally disordered structure and then to select from these a combination of possible structures to give the best agreement with the observed intensities of the diffuse reflections.

PREVIOUS WORK

Pauling (1930) put forward the general structural scheme for layer silicates, among them pyrophyllite. From powder diffraction patterns, Gruner (1934) found that pyrophyllite was monoclinic with cell dimensions $a = 5.14 \text{ \AA}$, $b = 8.90 \text{ \AA}$, $c = 18.55 \text{ \AA}$ and $\beta = 99.90^\circ$. He deduced that the space group was $C2/c$ and proposed a structure which gave reasonable agreement with his powder data. Hendricks (1938) used single crystal methods to examine pyrophyllite. He verified Gruner's cell dimensions finding $a = 5.15 \text{ \AA}$, $b = 8.88 \text{ \AA}$, $c = 18.60 \text{ \AA}$ and $\beta = 100.75^\circ$. The diffraction patterns showed the space group to be $C2/c$ or Cc . The single crystal data showed that the structure of the individual layers proposed by Gruner was essentially correct but that there was disorder in the superposition of the layers. Hendricks obtained co-ordinates for the atoms which agreed with the observed intensities for reflections with $k = 3n$. No structure compatible with the space group could be found when reflections with $k \neq 3n$ were considered.

EXPERIMENTAL

Many crystals of pyrophyllite from different sources were examined, without success, in an attempt to find an ordered crystal. All the crystals had about the same degree of structural disorder, but there were large differences in mechanical distortion, as shown by streaking of reflections into arcs. The specimen used for the structure determination was cut from a cleavage flake, elongated along the a -axis, of a sample from Graves Mountain, Georgia, obtained from Dr. R. C. Mackenzie, Macaulay Institute for Soil Research, Aberdeen. Chemical analysis of this material leads to the structural formula

$0.07 M^+ (Al_{3.91} Fe_{0.04} Mg_{0.01} Ca_{0.07}) (Si_{7.90} Al_{0.10}) O_{20} (OH)_4$ (Heller *et al.*, 1962). The crystal used for intensity measurements was $0.4 \times 0.4 \times 0.05$ mm. Cell dimensions were obtained from oscillation photographs taken in a single crystal camera with Straumanis-type film mounting using $CuK\alpha$ radiation. The camera was calibrated with powder photographs of silicon. Weissenberg photographs with multiple film packs (using $CuK\alpha$ radiation) were taken about the a -axis for levels with $h = -1, 0, 1$ and 2 and about the b -axis for levels with $k = 0, 1, 2, 3$ and 4 . The extension of the reflections along Debye-Scherrer arcs required the use of a wide aperture in the layer line screen to include all the diffracted intensity. $MoK\alpha$ radiation could not be used because the resolution was not adequate. The intensities were measured with a Joyce-Loebl microphotometer by integrating the intensity over the reflection and subtracting the intensity measured over a similar area of adjacent background. The observed intensities were corrected graphically for Lorentz and polarization factors but were not corrected for absorption although, with $\mu/\rho = 32$, absorption will not be negligible.

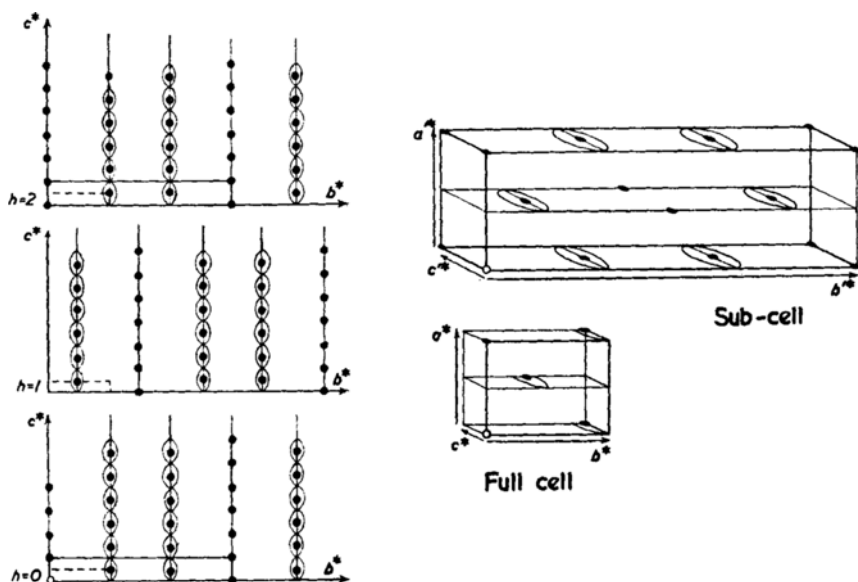


FIG. 1. A reciprocal space representation of X-ray diffraction from pyrophyllite.

Sharp reflections and maxima on streaks are shown by ●.

Streaks are shown by 

No attempt is made to show the degree of diffuseness of the streaks (see Table 1).

DESCRIPTION OF X-RAY PATTERNS

The X-ray reflections are distorted in two ways: by disorientation of the crystallites in each flake and by structural disorder. The first causes the reflections to be drawn out into arcs of constant θ and is an effect similar to that given by oriented aggregates of clays; the second causes reflections with $k \neq 3n$ to be streaked out in the c^* direction. In reciprocal space (Fig. 1), the intensity for these reflections is distributed along hk rods to a variable degree (Table 1) depending on the value of k . There is a marked tendency

TABLE 1.—NATURE OF PYROPHYLLITE REFLECTIONS

k	Nature of reflections	k	Nature of reflections
0	sharp	6	sharp
1	streaked	7	sharp
2	very streaked	8	very streaked
3	sharp	9	sharp
4	streaked	10	sharp
5	very streaked	11	very streaked?

for the hk rods to have intensity maxima where $l = 2m + 1$ and to fade to minima, or even zero, where $l = 2m$. The greater part of the scattered intensity is contained in the reflections with $k = 3n$.

SYMMETRY

Taking account of the sharp reflections and the intensity maxima of the diffuse reflections the unit cell is monoclinic with $a = 5.17 \text{ \AA}$, $b = 8.92 \text{ \AA}$, $c = 18.66 \text{ \AA}$ and $\beta = 99.8^\circ$. The systematic extinctions are hkl absent when $h + k$ is odd, $h0l$ absent when l is odd. The possible space groups are therefore $C2/c$ or Cc , which is in agreement with Hendricks (1938). In addition to these systematic absences there are additional non space group absences, viz. hkl reflections with $k = 3n$ are present only when l is even, and hkl with $k \neq 3n$ are present only when l is odd. This situation, in which there are systematic extinctions additional to those required by any space group, together with diffuseness of certain groups of reflections, is similar to what Kasper, Lucht and Harker (1950) found for decaborane, $B_{10}H_{14}$, which they treated as a partially disordered structure.

Following Kasper, Lucht and Harker (1950), it was decided to find the ideally disordered structure, which is represented by the subcell defined by the sharp reflections with $k = 3n$. This subcell has $a' = a = 5.17 \text{ \AA}$, $b' = b/3 = 2.97 \text{ \AA}$, $c' = c/2 = 9.33 \text{ \AA}$, $\beta' = \beta = 99.8^\circ$. In the subcell $h'k'l'$ are present when $h' + l'$ is even, $h'0'$ present when h' is even and $0k'0$ present when k' is even. This leads to possible space groups of $C2$, $C2/m$ or Cm for the subcell.

DETERMINATION OF THE STRUCTURE OF SUBCELL

Co-ordinates for the subcell were obtained starting from (1) the co-ordinates given by Wyckoff (1957), which are those for Gruner's (1934) structure, and (2) the co-ordinates obtained by twisting the tetrahedra in Wyckoff's structure through 9.5° as suggested by Radoslovich (1962).

The subcell co-ordinates were obtained by subtracting 0, or $1/3$ or $2/3$ from the y co-ordinates and 0 or $1/2$ from the z co-ordinates and rescaling to the subcell. After translating the y co-ordinates into the subcell, it was found that translation of the z co-ordinates generated no additional sites. The contents of the subcell, are given in Table 2.

TABLE 2.—ATOMIC CONTENTS AND SITES FOR PYROPHYLLITE IN $C2/m$ SUBCELL

Atom	Number	Site*
$2/3$ Al	2	(a)
$2/3$ Si	4	(i)
1 O(1)	4	(i)
$1/3$ O(2)	8	(j)
$1/3$ O(3)	4	(i)

* Nomenclature in *International Tables* (1952).

The space group of this subcell is $C2/m$, in agreement with the observed absences.

Using atomic scattering factors for fully charged atoms (*International Tables*, 1962) structure factors were calculated for (1) and (2) above. Structure (2) agreed much better with the observed values and was chosen for refinement.

REFINEMENT OF THE CO-ORDINATES

The a -axis and b -axis data have been refined separately to obtain the final co-ordinates. An attempt was made to put both sets on the same scale, but a satisfactory scaling factor could not be found. This might arise, for example, from differences in absorption for the two sets or from the different ways the arced reflections cut the sphere of reflection. Both sets of data refined toward the same co-ordinates.

Fourier and difference syntheses of the $h0l$ zone were made first. This projection was chosen because (1) the zone is composed of sharp reflections, unlike the $0kl$ where only $06l$ are sharp, and (2) the b -axis projection of the cell and the subcell are the same.

Satisfactory projections were obtained and Fig. 2 shows the Fourier and difference Fourier maps.

The $h0l$ (58 reflections) and the a -axis data (67 reflections) were then

refined by least squares, allowing Al, Si and O to have anisotropic temperature factors. The quantity

$$R_1 = \Sigma [|F_o(hkl)| - |F_c(hkl)|]^2$$

was minimized using a full matrix least-squares program (written for the purpose in Extended Mercury Autocode) on an ICT Orion computer. The observations were given equal weight and the scale factor was applied to F_c during refinement and applied to F_o at the end. The $h0l$ data were refined for scale factor, x and z co-ordinates for Si, O(1), O(2) and O(3). The a -axis data were refined for scale factor, y co-ordinate for O(2) (this is the only y co-ordi-

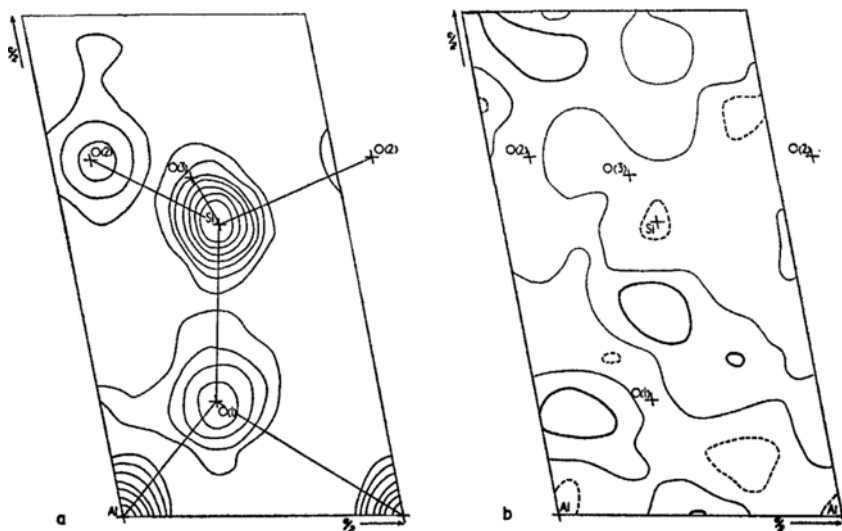


FIG. 2.(a) Electron density of pyrophyllite projected on (010). Contours are at equal arbitrary intervals. Crosses mark the positions of the atoms. This projection is the same for the ideally disordered subcell (when Al is 2/3 of an atom; Si, 2/3 atom; O(1), 1 atom; O(2), 2/3 atom; O(3), 1/3 atom) and for the full cell when each site represents three times as many atoms as in the subcell.

FIG. 2.(b) Electron density difference synthesis corresponding to Fig. 2a. The contour interval is half the interval on Fig. 2a. The thick continuous line denotes regions of positive electron density, the thin line is the zero contour and the broken line denotes negative regions.

nate not fixed by the space group) and z co-ordinates for Si, O(1), O(2) and O(3). The x co-ordinates were held at the values obtained from the $h0l$ refinement during the refinement of the a -axis data because of the limited range of h , up to 2 only, in the latter. The final R values were 0.180 for the $h0l$ zone and 0.148 for the a -axis data. These were considered satisfactory considering the poorly crystalline nature of pyrophyllite.

RESULTS

The fractional co-ordinates for the atoms in the subcell are given in Table 3 together with their estimated standard deviations. There are two estimates

TABLE 3.—ATOMIC CO-ORDINATES IN SUBCELL OF PYROPHYLLITE

	x		y		z					
	b -axis		a -axis		a -axis		b -axis		mean	
	x	$\sigma(x)$	y	$\sigma(y)$	z	$\sigma(z)$	z	$\sigma(z)$	z	$\sigma(z)$
2/3 Al	0	S.G.	0	S.G.	0	S.G.	0	S.G.	0	S.G.
2/3 Si	.2752	.0027	.5000	S.G.	.2920	.0016	.2926	.0018	.2923	.0009
1 O(1)	.2080	.0033	.5000	S.G.	.1151	.0024	.1171	.0018	.1161	.0012
1/3 O(2)	.0699	.0047	.1715	.0206	.3554	.0053	.3600	.0027	.3577	.0030
1/3 O(3)	.2410	.0125	0	S.G.	.3367	.0081	.3409	.0074	.3388	.0055

S.G. means co-ordinate fixed by space group.

$$\sigma(\text{mean}) = (\sqrt{[\sigma^2(a) + \sigma^2(b)]})/2.$$

for each of the z co-ordinates. When any one of a pair of estimates of z is compared with the other estimate and its standard deviation, it is within 1 standard deviation in six of the eight possible comparisons, and well within 2 standard deviations in all of them. Mean values for z were therefore taken and their standard deviations calculated.

Table 4 gives bond lengths and interatomic distances calculated from the co-ordinates of Table 3.

DISCUSSION

Figs. 2a and 3a illustrate the structure of the subcell. In Fig. 3a lines are drawn between oxygens on the surface of the layer, i.e. the O(2) and O(3) oxygens, to show the ways that the nearly equilateral triangular bases of Si—O tetrahedra can be completed from the available sites. The tetrahedra are seen to be twisted through an angle of 10° – 10.5° . In the ideal structure, one edge of the basal triads is parallel to the a -axis. Radoslovich (1962) predicted that the twist for pyrophyllite would be 9.58° . This calculation was based on $\text{Si—O}_{\text{surface}} = 1.60 \text{ \AA}$ and an average $\tau = \text{O}_{\text{apex}}\text{—Si—O}_{\text{surface}} = 109.47^\circ$, the angle for a regular tetrahedron. The average Si—O_{surface} found here is 1.606 \AA and this together with the observed twist, say 10.25° , leads to $\tau = 109.76^\circ$, very close to the value for a regular tetrahedron. Fig. 3b shows the three different ways of choosing tetrahedral networks. The array of surface oxygens in each network is clearly ditrigonal. Each network forms tetrahedra around two of every three Si sites and leaves the other Si site about 2.37 \AA from the nearest oxygens. Similarly each network uses

TABLE 4.—BOND LENGTHS AND INTERATOMIC DISTANCES IN Å

		Length	σ	
Tetrahedron				
(filled by Si)	Si—O(1) apex	1.622	0.020	
	Si—O(2)	1.622	0.044	
	Si—O(2)	1.629	0.043	
	Si—O(3)	1.568	0.018	
	Si—O mean	1.610	0.017	
	O(1)—O(2)	2.652		
	O(1)—O(2)	2.713		
	O(1)—O(3)	2.538		
	O(2)—O(2)	2.628		
	O(2)—O(3)	2.630		
	O(2)—O(3)	2.610		
O—O mean	2.628			
Octahedron				
(2/3 filled with Al)	Al—O(1) parallel to (010)	2.002		
	Al—O(1)	2.036		
	Al—O mean	2.025		
	O(1)—O(1) parallel to <i>b</i>	2.974		} In (001) plane } Inclined to (001) plane
	O(1)—O(1)	2.982		
	O(1)—O(1)	2.781		
O(1)—O(1) parallel to (010)	2.723			
Interlayer contacts	O(2)—O(2)	2.890	0.038	} 1 Chain parallel to the <i>a</i> -axis } 2 Chains inclined $\pm 120^\circ$ to the <i>a</i> -axis
	O(2)—O(2)	3.028		
	O(2)—O(3)	3.009	0.058	
	O(2)—O(2)	3.066		
	O(3)—O(3)	3.343		

only one out of every three surface oxygen sites. Hence the occupancy in the subcell of each Si site by 2/3 silicon atom and of each O(2) and O(3) site by 1/3 oxygen atom.

Table 4 shows bond lengths and interatomic distances. The bond lengths in the Si—O tetrahedron have no unexpected features. The average Si—O bond length, 1.610 Å, is close to the average value reported by Smith and Bailey (1963) for these bonds in layer silicates and is within one standard deviation of their recommended value of 1.620 Å. The average O—O contact along the edge of the tetrahedron is 2.627 Å, which is close to the average value, 2.634 Å, for forty-eight edges of tetrahedra measured by Megaw, Kempster and Radoslovich (1962) for anorthite and 2.643 Å for similar edges in dickite (Newnham, 1961). The bond Si—O(1), i.e. to the apical oxygen, makes an angle of 2.4° with the normal to (001) plane; the plane of the surface oxygens is tilted 4.1° from the (001) plane. From the standard deviations of the distances involved, these tilts, with $\delta l/\sigma = 3.0$ and 4.7 respectively, are both significant.

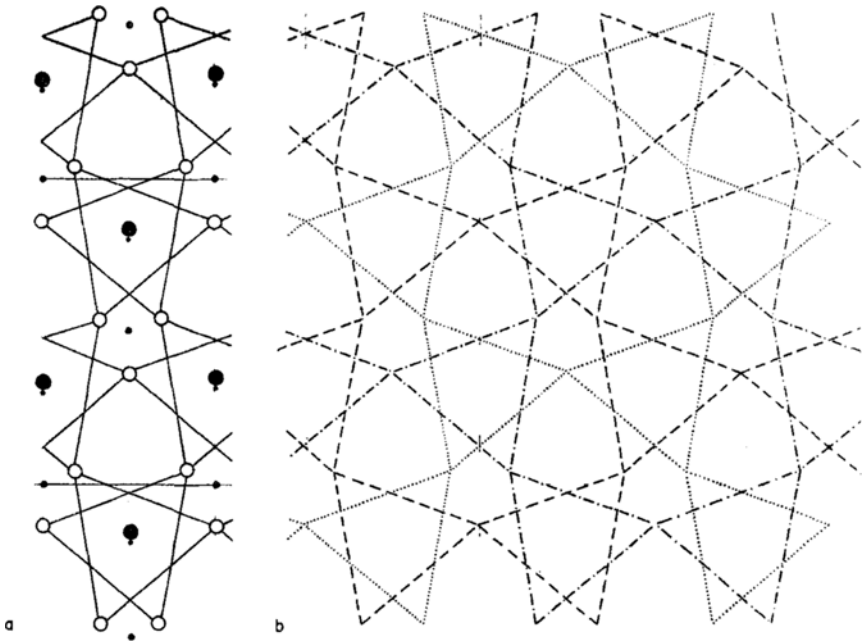


FIG. 3.(a) Positions of atoms in pyrophyllite viewed normal to the layers for the portion of the structure between $z = 0$ and $z = 1/2$ in the subcell.

- $2/3$ Al at $z = 0$
- $2/3$ O + $1/3$ OH at $z = 0.116$
- $2/3$ Si at $z = 0.292$
- $1/3$ O at $z \approx 0.35$

The lines pick out the bases of tetrahedral groups of oxygens.

FIG. 3.(b) The three possible linked networks of tetrahedral groups (represented by their bases) in three adjacent subcells of pyrophyllite. Only one of these networks can be occupied in any single layer of tetrahedra.

Individual Al—O or O—O distances in the octahedral layer of pyrophyllite cannot be obtained from our results. The dimensions determined from the subcell structure are the average of one vacant and two occupied octahedra. The average distance for the $2/3$ Al site—O should be compared with the weighted mean distance for the two occupied octahedra and one empty octahedron in muscovite. The distances are 2.025 Å in pyrophyllite and, according to Radoslovich (1963), 2.037 Å in muscovite and this, together with the comparison of octahedral O—O separations in pyrophyllite, muscovite (Radoslovich, 1960) and dickite (Newnham, 1961) in Table 5, shows that the octahedral layers in pyrophyllite and muscovite are very similar and significantly thicker than in dickite.

TABLE 5.—AVERAGE OCTAHEDRAL DISTANCES IN Å IN PYROPHYLLITE, MUSCOVITE AND DICKITE

	Distance, Å		
	Pyrophyllite	Muscovite	Dickite
O—O parallel to layers	2.979	2.996	2.997
O—O inclined to layers	2.762	2.767	2.685
O—O average overall	2.871	2.881	2.841
Layer thickness	2.135	2.12	2.06

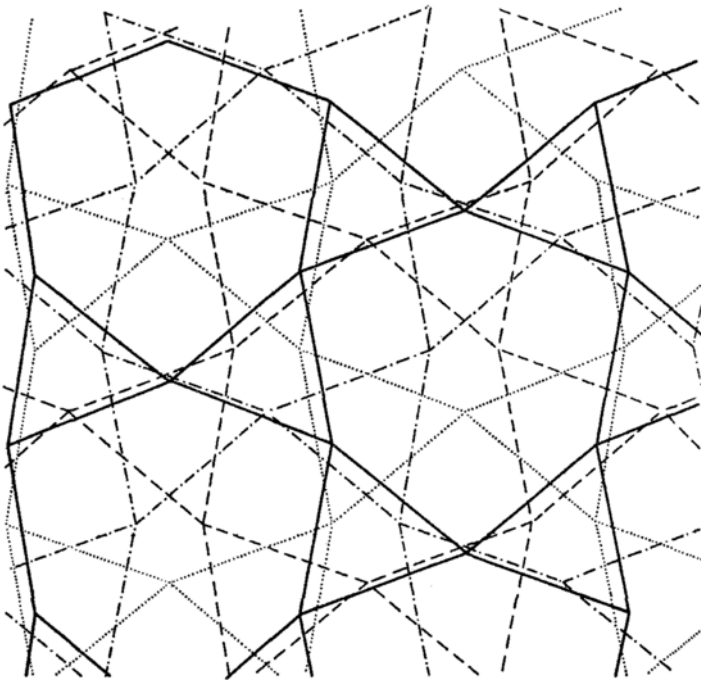


FIG. 4. Interlayer oxygen contacts in pyrophyllite. One of the three possible networks of tetrahedra on the lower surface of one layer ($z \approx 0.65$) indicated by the continuous line is shown superposed on the three possible networks on the upper surface (indicated by the three different kinds of broken line) of the adjacent layer ($z \approx 0.35$).

Fig. 4 shows the three possible ways in which the surface oxygen networks of adjacent layers can come together. Only one of the three possible networks for the upper layer is drawn on the figure; the other two give similar O—O contacts. However, the other arrangements are different with respect to the fixed symmetry elements of the full unit cell. In two of the three possible

arrangements in Fig. 4, parallel chains of O—O contacts make angles of about $\pm 120^\circ$ with the *a*-axis. These two have the same sequence of O—O contact distances along the chains viz. 3.009 Å, 3.066 Å, 3.009 Å, 3.343 Å, 3.009 Å. . . The other arrangement has chains of contacts that are parallel to the *a*-axis. The sequence of O—O distances along these chains is 3.028 Å, 2.890 Å, 3.028 Å. . . With one possible exception, these are reasonable for unbonded contacts. This distance, 2.890 Å is, shorter than the OH—O inter-layer contacts in dickite 2.94 Å, 2.97 Å and 3.12 Å, which are generally thought to be OH—O bonds. It may be, therefore, that the arrangement with short O—O contacts is not favored in the structure.

REFERENCES

- BROWN, B. E., and BAILEY, S. W. (1963) Chlorite polytypism, II, Crystal structure of a one-layer Cr-chlorite, *Am. Mineralogist* **48**, 42–61.
- DRITS, V. A., and KASHABV, A. A. (1960) An X-ray study of a single crystal of kaolinite, *Soviet Phys.-Cryst.* **5**, 207–10.
- GRUNER, J. W. (1934) The crystal structure of talc and pyrophyllite, *Z. Krist.* **88**, 412–9.
- HELLER, L., FARMER, V. C., MACKENZIE, R. C., MITCHELL, B. D., and TAYLOR, H. F. W. (1962) The dehydration and rehydroxylation of trimorphic dioctahedral clay minerals, *Clay Minerals Bull.* **5**, 56–72.
- HENDRICKS, S. B. (1938) On the crystal structure of talc and pyrophyllite, *Z. Krist.* **99**, 264–74.
- HENDRICKS, S. B. (1940) Variable structures and continuous scattering of X-rays from layer silicate lattices, *Phys. Rev.* **57**, 448–54.
- International Tables for X-ray Crystallography* (1952) pp. 52 and 95, vol. 1, Kynoch Press, Birmingham.
- International Tables for X-ray Crystallography* (1962) p. 201, vol. 3, Kynoch Press, Birmingham.
- KASPER, J. S., LUCHT, C. M., and HARKER, D. (1950) The crystal structure of decaborane, $B_{10}H_{14}$, *Acta Cryst.* **3**, 436–55.
- MATHIESON, A. McL. (1958) Mg-vermiculite, a refinement and re-examination of the crystal structure of the 14.36 Å phase, *Am. Mineralogist* **43**, 216–27.
- MATHIESON, A. McL., and WALKER, G. F. (1954) Crystal structure of Mg-vermiculite, *Am. Mineralogist* **39**, 231–55.
- MEGAW, H. D., KEMPSTER, C. J. E., and RADOSLOVICH, E. W. (1962) The structure of anorthite, $CaAl_2Si_2O_8$, II, Description and discussion, *Acta Cryst.* **15**, 1017–35.
- MORIMOTO, N., DONNAY, G., TAKEDA, H., and DONNAY, J. D. H. (1963) Crystal structure of synthetic iron mica (abstract), *Acta Cryst.* **16** (Suppl.), A 14.
- NEWNHAM, R. E. (1961) A refinement of the dickite structure and some remarks on the polymorphism of the kaolin minerals, *Mineral. Mag.* **32**, 683–704.
- NEWNHAM, R. E., and BRINDLEY, G. W. (1956) The crystal structure of dickite, *Acta Cryst.* **9**, 759–64.
- PAULING, L. (1930) The structure of micas and related minerals, *Proc. Nat. Acad. Sci., U.S.* **16**, 123–9.
- RADOSLOVICH, E. W. (1960) The structure of muscovite $KAl_2(Si_3Al)O_{10}(OH)_2$, *Acta Cryst.* **13**, 919–32.
- RADOSLOVICH, E. W. (1962) The cell dimensions and symmetry of layer-lattice silicates, II, Regression relations, *Am. Mineralogist* **47**, 617–36.
- RADOSLOVICH, E. W. (1963) The cell dimensions and symmetry of layer-lattice silicates, IV, Interatomic forces, *Am. Mineralogist* **48**, 76–99.

84 THIRTEENTH NATIONAL CONFERENCE ON CLAYS AND CLAY MINERALS

- SMITH, J. V., and BAILEY, S. W. (1963) Second review of Al—O and Si—O tetrahedral distances, *Acta Cryst.* **16**, 801–11.
- STEINFINK, H. (1958a) The crystal structure of chlorite, I. A monoclinic polymorph, *Acta Cryst.* **11**, 191–5.
- STEINFINK, H. (1958b) The crystal structure of chlorite, II. A triclinic polymorph, *Acta Cryst.* **11**, 195–8.
- STEINFINK, H. (1962) The crystal structure of a trioctahedral mica, phlogopite, *Am. Mineralogist* **47**, 886–96.
- STEINFINK, H., and BRUNTON, G. (1956) The crystal structure of amesite, *Acta Cryst.* **9**, 487–92.
- TAKÉUCHI, Y., and SADANAGA, R. (1959) The crystal structure of xanthophyllite, *Acta Cryst.* **12**, 945–6.
- WYCKOFF, R. W. G. (1957) *Crystal Structures*, p. 67, ch. XII, vol. III, Interscience, New York.